Amination of dimethyl ether on zeolite catalysts. 2. Acidic properties of the used T-zeolites and their influence on the catalytic reaction

A. Martin *, H. Berndt, U. Wolf and B. Lücke

Zentrum für Heterogene Katalyse, Rudower Chaussee 5, O-1199 Berlin, Germany

Received 18 February 1992; accepted 28 April 1992

Freshly prepared and used H/Na, K–T-zeolite catalysts for the conversion of dimethyl ether and ammonia to the three methylamines have been characterized by temperature-programmed desorption of ammonia and IR spectroscopy. Activity and selectivity depend on the nature and number of the acid sites. With time on-stream, deep alterations in the catalyst behaviour have been observed. The activity of the catalyst is decreased by blocking of active sites ≈ 5–10 h: furthermore, during an initial period hydrocarbons were formed almost exclusively on strong-acid sites. A second period is characterized by an increased "shape selectivity" observed in the distribution of the methylamines. The amination will proceed probably on left weak-acid sites and on the outer surface in a third period, however, without "shape selectivity" due to the progressive blocking of the inner catalyst surface.

Keywords: Dimethylether amination; methylamines; zeolite T; acidic properties; TPDA; IR spectroscopy

1. Introduction

Methylamines (MA) are commercially produced from methanol (MeOH) and ammonia (NH_3), normally by a vapour-phase heterogeneous process on solid acid catalysts such as amorphous silica–alumina, at ≈ 673 K and under a pressure of 1.5–3 MPa [1,2]. Shifts in the product distribution, particularly to enhance the dimethylamine (DMA) yield, are important, and extensive studies have been done by application of zeolite catalysts (e.g., refs. [3–5] and references therein), including efforts to commercialize the zeolite-catalyzed process (e.g., ref. [6]).

* To whom correspondence should be addressed.

Recently, we reported on the formation of MA by passing dimethyl ether (DME) and NH_3 as feed over erionite-rich T-zeolites as catalysts [7]. We observed a significant influence of the concentration of acid sites of the T-zeolites on the catalytic activity and on the MA distribution. In principle, with increasing exchange of alkali cations for protons the formation of hydrocarbons will be enhanced, especially in the temperature region above 673 K. Moreover, the alkali cations significantly influence the distribution of MA by pore narrowing. The MA distribution data found by application of the T-zeolites was the same as reported for erionite-like materials using MeOH as feed [3,8,9].

In this work we report on the characterization of the nature and concentration of acid sites of the catalysts by temperature-programmed desorption of ammonia and IR-spectroscopic investigations, and on their role in the amination reaction. Recently, we have observed that a high proton content leads to an enhanced formation of hydrocarbons combined with a rapid deposition of carbonaceous products blocking the narrow pores. Otherwise, the blockage of Brønsted sites should have a promoting effect on the formation of MA. For better understanding we performed long-duration experiments with a selected catalyst sample to observe the catalyst ageing, particularly to obtain information about the time-dependent changes in selectivity.

2. Experimental

2.1. CATALYST PREPARATION AND REACTION DEVICE

The applied T-zeolite, a structural intermediate of erionite and offretite, was synthesized under conditions which favour the formation of erionite (Si-to-Al ratio of ≈ 4.2, crystallite size of 2–3 μm). Three zeolite samples (described as TB, TC and TD) with different H^+-to-Na^+/K^+ ratios were prepared. Additionally, the as-synthesized form of the zeolite (sample TA) was included in the investigations. The exchange procedure (0.5 N NH_4NO_3, 353 K) and pretreatment conditions (35 wt% SiO_2 as binder), as well as the catalytic apparatus and reaction parameters have been described elsewhere [7]. The long-duration experiment (30 h, sample TD) was carried out under the same reaction conditions. Table 1 contains some characteristics of the samples used for the studies.

2.2. CATALYST CHARACTERIZATION

The acid sites of the catalysts were characterized by well-established methods, such as temperature-programmed desorption of ammonia and IR spectroscopy [10].

Table 1
Catalyst pretreatment, alkali-ion amount and proton content evaluated from the alkali-ion exchange

Catalyst sample	Exchange time (h)	Na^+/K^+-content (wt% Na_2O)	H^+-content (mmol H^+/g)
TA	–	8.8	0
TB	2	4.9	1.26
TC	8	2.8	1.94
TD	16 [a]	1.0	2.52

[a] Intermediate calcination at 773 K after every fourth hour of exchange time.

IR spectroscopy

The customary pyridine adsorption technique could not be used because of the small diameter of the pores of the erionite-like material. Thus, we have used NH_3 as probe to determine Brønsted sites (BS) and Lewis sites (LS) [11]. The investigations were carried out on a Bruker IFS 66 FTIR-spectrometer using self-supporting wafers with a diameter of 20 mm and a weight of 30 mg. The spectra were recorded in the region of 1200–4000 cm^{-1}, wherein the NH_3 adsorption bands could be observed in the 1300–1700 cm^{-1} region and the OH-stretching vibrations between 3500 and 3800 cm^{-1}. Furthermore, we used IR spectroscopy to distinguish between weak-acid Brønsted sites (WBS) and strong-acid Brønsted sites (SBS) after an intermediate heating of the samples. The base spectra were obtained after NH_3 adsorption and evacuation at 298 K. Then the samples were heated up to 593 K (10 K/min). The temperature was kept ≈ 40 min under subsequent evacuation, and the next spectra recorded after cooling to RT showed only the NH_3 adsorption on the SBS. The difference of the two curves stands for NH_3 adsorption on the WBS.

Temperature-programmed desorption of ammonia (TPDA)

The TPDA was carried out in a conventional flow system with a thermal conductivity detector (TCD). However, the narrow pore system of these catalysts requires special investigation conditions to ensure that a quantitative elution of physisorbed NH_3 is reached, the low-temperature peak (LTP) and the high-temperature peak (HTP) are separated. The amount of NH_3 desorbed was also determined by volumetric analysis after absorption in 0.025 N H_2SO_4. Samples of 150 mg of catalyst each were placed in a U-tube reactor. Adsorbed water was removed for 1 h by heating the samples to 673 K (10 K/min) under flowing helium (2.5 ℓ/h). After cooling to 373 K, the samples were saturated with NH_3 by passing a helium stream (2.5 ℓ/h) containing 2.7 vol% NH_3 for 20 min. Then the physisorbed NH_3 was removed with a helium flow at 393 K for 2 h. In order to monitor the separate desorption of NH_3 bound on the weak and strong acid sites the following four-step TPDA option was applied:

(1) Temperature ramp from 373 to 573 K (10 K/min).

(2) Isothermal step at 573 K for 1.5 h to complete the desorption and elution of the LTP-NH_3.

(3) Temperature ramp from 573 to 873 K (10 K/min).

(4) Isothermal step at 873 K for 1 h to complete the desorption and elution of all the HTP-NH_3 out of the pore system.

The temperature of the first isothermal step has been selected from a TPDA experiment by continuously increasing the desorption temperature from 373 up to 873 K (10 K/min). The LTP maximum was found at about 483 K. In the four-step programme a temperature higher by 90 K was used to complete the LTP-desorption process which is limited by the diffusion of the NH_3 molecules through the pore system of the narrow-pore material. Using this procedure the desorption of the HTP-NH_3 started only at 653 K.

3. Results and discussion

Fig. 1 shows the IR spectra of the catalysts TA–TD in the region of 1300–1700 cm^{-1} obtained with ammonia as probe molecule. The spectral band

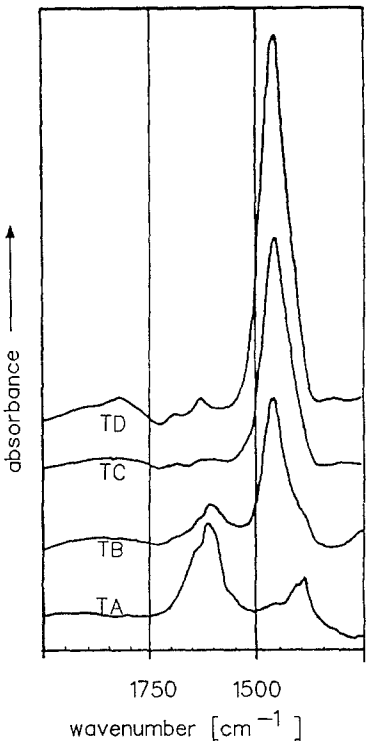

Fig. 1. IR spectra of T-zeolites with different alkali-cation content (TA–TD) after ammonia adsorption and evacuation at RT (20 min, 10^{-3} Pa).

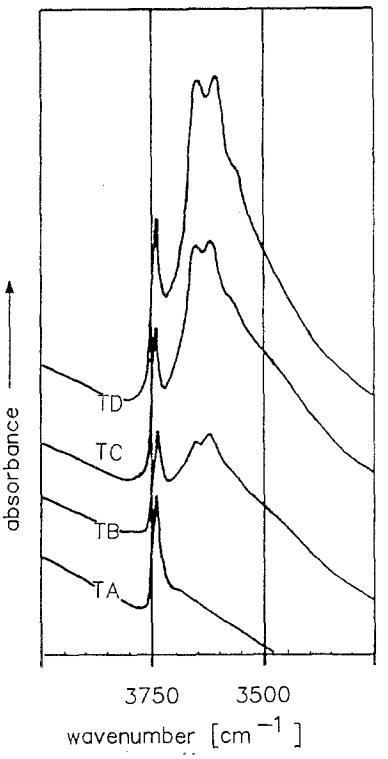

Fig. 2. IR spectra of T-zeolites TA–TD in the OH stretching vibration region after evacuation at 673 K (1 h, 10^{-3} Pa, recorded at RT).

of the BS is given at 1455 cm^{-1}, while the band characterizing the LS is given at 1625 cm^{-1} with an additional small signal at $\approx$ 1390 cm^{-1}. The characteristic bands for the LS could be observed only on sample TA. These LS could be due to non-framework aluminium left after the zeolite synthesis and located into the pore system or on the outer surface. Furthermore, it could be possible that the LS observed should be attributed to the generation of such sites by alkali-cation covered BS (e.g., refs. [12,13] and references therein) or to "true" LS [14,15]. In the first case, we should find a decline in the intensities of these bands with increasing proton content and in the latter case the "true" LS should be maintained without changing. In the spectra of the proton-containing samples (TB–TD), however, further clearly indicated bands which could be attributed to the LS have not been observed. Thus, we suppose that the observed LS of the sample TA could be assigned to non-framework aluminium which was removed by the first exchange procedure.

As expected, the Brønsted acidity (band at 1455 cm^{-1}) is enhanced with increasing H^+-content (samples TB–TD). Fig. 2 reflects the OH-band region (3500–3800 cm^{-1}) of the investigated samples. While we observed only weak-acid

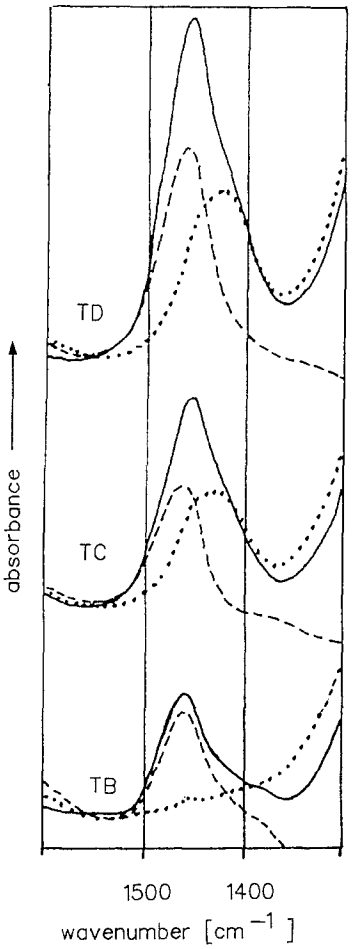

Fig. 3. IR spectra of T-zeolites TB–TD after ammonia adsorption. Curve a (———) after evacuation at RT (20 min, 10^{-3} Pa), curve b (· · · · · ·) after evacuation at 593 K (40 min, 10^{-3} Pa, recorded at RT), curve c (- - - - - -) difference between the spectra a and b.

OH groups on sample TA (band at 3742 cm^{-1}), we found an increase of the bands at 3660 and 3610 cm^{-1} (on samples TB–TD) characterizing BS.

Fig. 3 depicts the separation of the WBS and SBS by desorption of NH_3 adsorbed on the WBS at 593 K on the samples TB–TD. The spectra of NH_3 adsorbed at RT (curve a) show one band at 1455 cm^{-1} for the BS. After heating the samples to 593 K, the weaker bound ammonia was desorbed and a band at 1430 cm^{-1} (curve b) could be observed characterizing SBS for the rest. The difference of the spectra (curve c) shows the share of the WBS with a band at 1465 cm^{-1}.

The results of the TPDA are demonstrated in figs. 4a and 4b. With increasing H^+-content the NH_3 desorbed from the SBS (HTP) and also the one desorbed

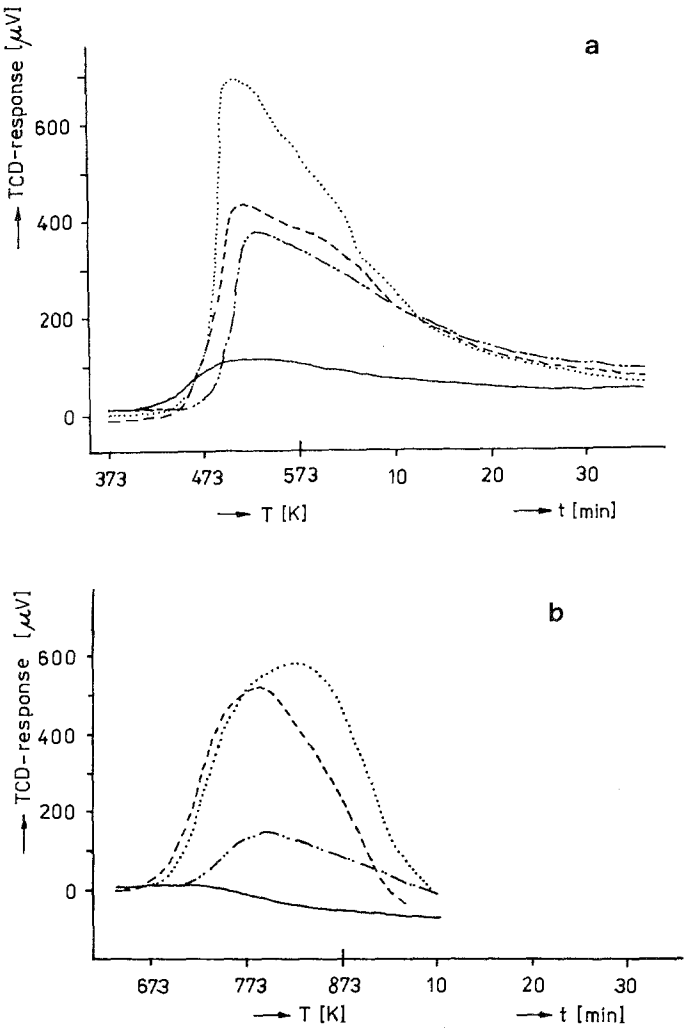

Fig. 4. TPDA spectra of the samples TA (———), TB (· · – · ·), TC (- - - - -) and TD (· · · · · ·) obtained with the four-step programme. (a) Desorption of LTP-NH_3 during steps 1 and 2. (b) Desorption of HTP-NH_3 during steps 3 and 4.

from the WBS (LTP) enhanced. Coherence has been obtained between the total amount of NH_3 determined by volumetric analysis and the H^+-content estimated from the alkali-ion exchange (table 1). Thus, the NH_3 desorbed in the LTP region has to be attributed to WBS for the samples TB–TD.

Therefore, fig. 5a mirrors this linear correlation between the degree of the alkali-ion exchange and the total amount of NH_3 desorbed and analyzed volumetrically. It is not surprising that the curve does not pass the origin (value for sample TA). This could be attributed to NH_3 adsorbed on the small amount of LS proved by IR spectroscopy. The different rising trend of the LTP-NH_3 and HTP-NH_3 curves corresponds to the different exchange behaviour of WBS

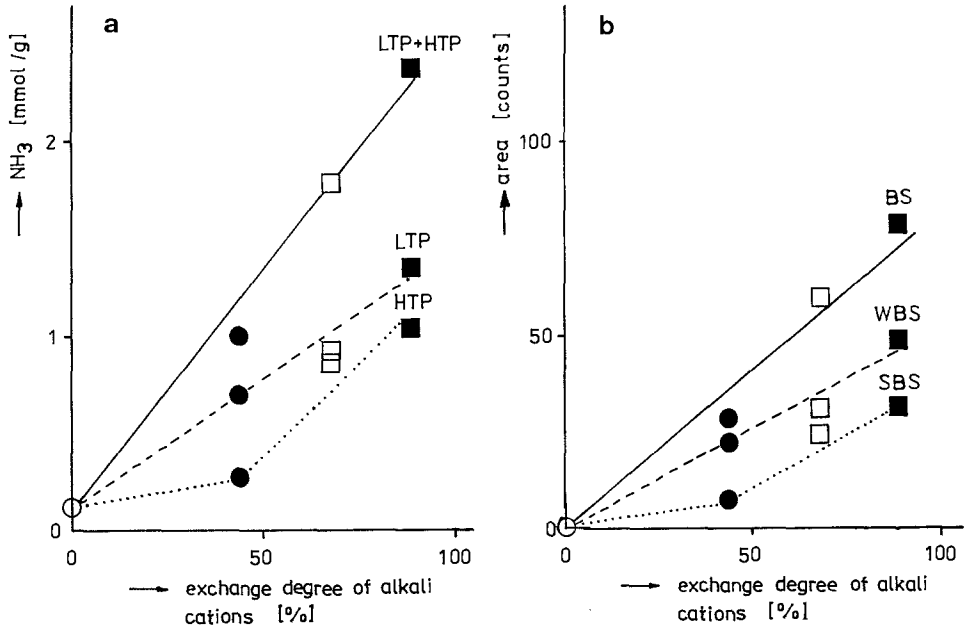

Fig. 5. Relation between the exchange degree of alkali cations and ammonia adsorbed on the samples TA (○), TB (●), TC (□) and TD (■). (a) Volumetric analysis of the LTP-NH_3 and HTP-NH_3. (———) LTP+HTP, (· · · · · ·) HTP, (- - - - - -) LTP. (b) Area of the IR band between 1350 and 1550 cm^{-1} (obtained from fig. 3). (———) IR band area of Brønsted sites (BS), (· · · · · ·) IR band area of strong-acid Brønsted sites (SBS), (- - - - - -) IR band area of the weak-acid Brønsted sites (WBS).

and SBS [16,17]. The alkali cations located on the WBS are exchanged faster than the alkali cations on the SBS. However, the number of the different kinds of acid sites enlarges with prolonging of the exchange time as well as by intermediate calcination.

Fig. 5b shows the quantitative relations of the IR-spectroscopic investigations for the separation of the two types of BS (spectra demonstrated in fig. 3). It has been clearly shown that the same relation was found in comparison with the TPDA measurements.

Considering the determination of the different acid sites the results of the catalytic investigations [7] can be discussed in more detail. On the sample TA (as-synthesized form) only a low DME conversion has been observed. Furthermore, the MA selectivity was nearly constant with increasing reaction temperature. High alkali-cation content corresponds to low H^+-content and leads to a low reaction rate. Then the product distribution is kinetically controlled up to the equilibrium point determined by the residence time available. On the exchanged samples TB–TD the DME conversion approaches 100%. The MA selectivity decreases drastically with rising temperature and increased concentration of acid sites of the samples (table 2). The DME cleavage necessary to form

Table 2
Methylamine selectivity S(MA) (NH_3-to-DME ratio = 2, WHSV = 0.5 h^{-1}, atmospheric pressure, 90 min on-stream) in dependence on the reaction temperature and number of LTP-NH_3 and HTP-NH_3

Catalyst sample	S(MA) (wt%)			LTP-NH_3 (mmol/g)	HTP-NH_3 (mmol/g)
	623 K	653 K	683 K		
TA	71	73	73	0.13	0
TB	97	95	86	0.70	0.3
TC	96	91	78	0.92	0.88
TD	89	82	44	1.36	1.03

methyl cations for the MA formation is overlapped by ether dehydration on SBS forming hydrocarbons.

Considering this, it seems that only a small amount of BS is sufficient for the alkylation of NH_3. The enlargement of the SBS amount leads to a decline of MA selectivity and to an enhanced formation of hydrocarbons.

In order to investigate the influence of the different acid sites on the catalytic properties, a long-duration MA synthesis on the sample TD was carried out. This experiment showed several changes in the first 10 h on-stream.

Fig. 6 depicts the conversion of DME and the yields of the by-products MeOH and hydrocarbons. Starting at $\approx 95\%$, the conversion showed a decrease to $\approx 65\%$ after 5–10 h on-stream. This decline occurs when the deposition of carbonaceous products on the catalyst has reached the reactor outlet. Then, the conversion remained nearly constant. Hence, the DME conversion is not further

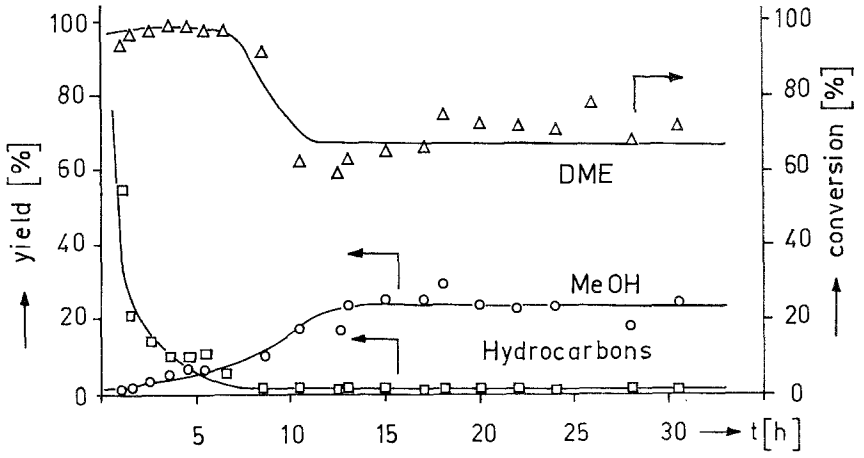

Fig. 6. Conversion of DME and yields of the by-products methanol and hydrocarbons (wt%) on sample TD in dependence on the reaction time (673 K, ammonia-to-DME ratio = 2, WHSV = 0.5 h^{-1}, atmospheric pressure).

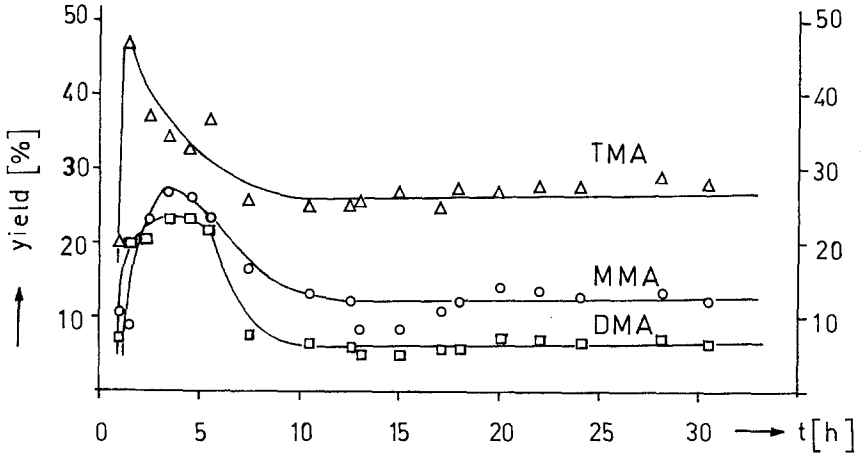

Fig. 7. Yields of MMA, DMA and TMA (wt%) on sample TD in dependence on the reaction time (673 K, ammonia-to-DME ratio = 2, WHSV = 0.5 h^{-1}, atmospheric pressure).

influenced by a progressive coking and blockage of the zeolite pores after ≈ 10 h on-stream. Hydrocarbons are the main reaction product over nearly 3 h due to the DME dehydration on the SBS according to the MTG-reaction type. The yield of hydrocarbons declined very rapidly by the blockage of the SBS by deposited "coke", as described elsewhere for the MTG-reaction on narrow-pore zeolites (e.g., ref. [18]), and therefore, the DME cleavage becomes predominant. The MA fraction raises to be the main product and we found an increased MeOH yield. The reason for this result is assumed to be the rapid blockage of the SBS connected with a change in the reaction pathways of the reaction of DME.

Furthermore, it is possible to divide the first five hours on-stream into three consecutive periods of catalyst alteration, which are reflected by the changes of the MA (fig. 7) and by-product yields (fig. 6). During the first conditioning period the MA fraction yield increased very rapidly. The second period (2–4 h) should be characterized by a distinct "shape-selective" effect due to a progressive coking and narrowing of the pore mouths. As a result, a decrease in the trimethylamine (TMA) yield and, consecutively, an increasing DMA and monomethylamine (MMA) amount was observed. Otherwise, in this period with increased coke formation the number of sites responsible for the methyl cation formation is more and more blocked and therefore the selectivity is shifted from TMA to DMA/MMA. The deactivation in the third period (from ≈ 5 h on) is connected with the decline in conversion of DME. With the blockage of the inner surface by coke and coke-precursor products the reaction proceeds on the outer surface increasingly without any changes in the MA fraction as normalized data proved.

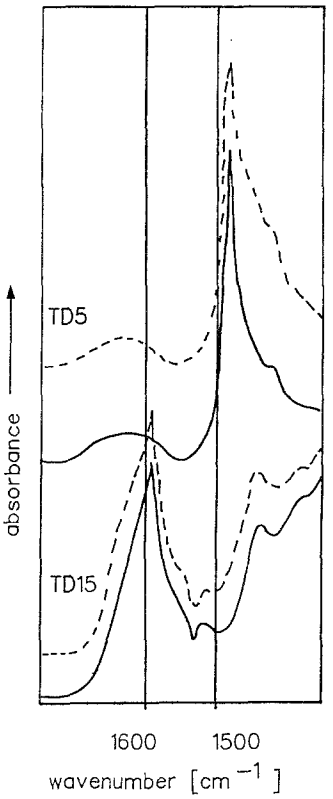

Fig. 8. IR-spectra of catalyst probes TD5 and TD15. (———) After evacuation and heating to 673 K for 1 h at RT, (- - - - -) after ammonia adsorption and evacuation at RT.

During the 30 h catalyst run, catalyst probes of different deactivation states from the catalyst bed were isolated. The characterization of these probes by TPDA and IR spectroscopy should give a better understanding of the role of the active sites (WBS and SBS) during the reaction.

It has been shown that two different probes (TD5 – after 5 h; TD15 – after 15 h) represent two states of alteration. Visually, TD5 only had a light brown coating, whereas TD15 was coked with a dark brown color.

Fig. 8 shows the IR spectra of probes TD5 and TD15. On TD5 a strong band in the spectra at ≈ 1480 cm^{-1} was observed which does not disappear during heating to 673 K. This band could be assigned to NH-deformation vibrations of N-containing compounds or "precoke". Furthermore, the band of the ammonia adsorbed on possible BS is overlapped by this "precoke" band. The spectra of TD15 do not reveal NH_3 adsorption due to the nearly total blockage of the acid sites by "coke", as indicated by the strong band at 1590 cm^{-1}.

The WBS of TD5 supposed could be indicated clearly by the difference in the spectra, however, possible SBS could also be observed as shoulder (fig. 9).

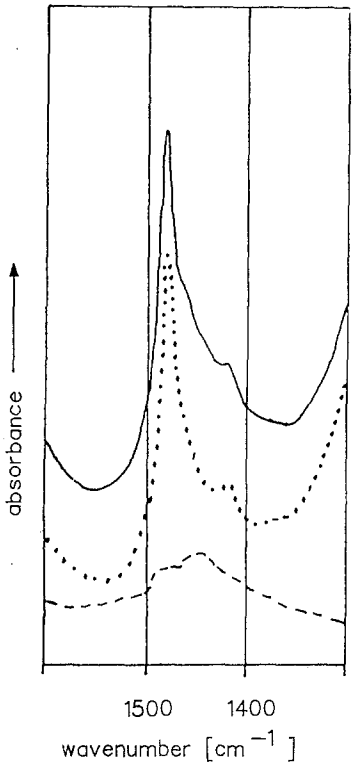

Fig. 9. Spectra of TD5 after ammonia adsorption. Curve a (———) after evacuation at RT (20 min, 10^{-3} Pa), curve b (· · · · · ·) after evacuation at 593 K (40 min, 10^{-3} Pa), curve c (- - - - - -) difference between the spectra of a and b.

In the TPDA only the LTP could be recorded clearly by TCD whereas the desorption of the HTP-NH_3 is overlapped by the decomposition of "coke" or the formation of organic products from "precoke". The amount of NH_3 determined by trapping and subsequent volumetric analysis can be solely used for the estimation of the amount of accessible SBS because basic N-containing compounds cause an overdetermination of the HTP-NH_3 desorbed from TD5. The TPDA data of TD5 show that there is after 5 h on-stream a loss of $\approx 15\%$ of WBS and $\approx 30\%$ of SBS at least compared with the fresh sample TD. On probe TD15 we found only 5% of WBS left compared to the amount of TD. The block of the narrow pores led to nearly complete unaccessibility of the inner surface and consequently, of the two types of BS too. However, on TD5 the amount of SBS is decreased comparatively more than that of WBS.

In conclusion, strong-acid sites are not favourable for the synthesis of MA. The catalysts best suited for this reaction are narrow-pore zeolites with only weak-acid sites: the strong-acid sites should be blocked with cations or by defined coating with coke using suitable catalyst pretreatments.

Acknowledgement

The authors thank Mrs. H. French for her assistance with the experimental work and Mrs. G. Keller for carrying out the TPDA measurements.

References

[1] *Ullmanns Encyclopädie der technischen Chemie*, Vol. 16 (Verlag Chemie, Weinheim, 1978) p. 671.
[2] J. Ramioulle and A. David, Hydrocarbon Process. 7 (1981) 113.
[3] M. Keane Jr., G.C. Sonnichsen, L. Abrams, D.R. Corbin, T.E. Gier and R.D. Shannon, Appl. Catal. 32 (1987) 361.
[4] W. Hölderich, M. Hesse and F. Näumann, Angew. Chem. Int. Ed. Engl. 27 (1988) 226.
[5] W. Hölderich, in: *Introduction to Zeolite Science and Practice*, Studies in Surface Science and Catalysis, Vol. 58, eds. H. van Bekkum, E.M. Flanigen and J.C. Jansen (Elsevier, Amsterdam, 1991) p. 702.
[6] Y. Ashina, T. Fujita, M. Fukatsu, K. Niwa and J. Yagi, in: *New Developments in Zeolite Science and Technology*, Studies in Surface Science and Catalysis, Vol. 28, eds. Y. Murakami, A. Iijima and J.W. Ward (Kodansha/Elsevier, Tokyo/Amsterdam, 1986) p. 779.
[7] A. Martin, B. Lücke, W. Wieker and K. Becker, Catal. Lett. 9 (1991) 451.
[8] U. Dingerdissen, Ph.D. Thesis, Darmstadt, Germany (1990).
[9] C. Herrmann, F. Fetting and C. Plog, Appl. Catal. 39 (1988) 213.
[10] J.A. Rabo and G.J. Gaida, Catal. Rev.-Sci. Eng. 31 (1989/90) 385.
[11] J.B. Peri, in: *Catalysis – Science and Technology*, Vol. 5, eds. J.R. Anderson and M. Boudart (Akademie-Verlag, Berlin, 1984) p. 171.
[12] J.W. Ward, Colloid Interface Sci. 28 (1968) 269.
[13] H.G. Karge and H.K. Beyer, in: *Zeolite Chemistry and Catalysis*, Studies in Surface Science and Catalysis, Vol. 69, eds. P.A. Jacobs, N.I. Jaeger, L. Kubelková and B. Wichterlova (Elsevier, Amsterdam, 1991) p. 43.
[14] G.H. Kühl, in: *Proc. 3rd Int. Conf. on Molecular Sieves, Recent Progress Reports*, ed. J.B. Uytterhoeven (Univ. Leuven Press, Leuven, 1973) paper No. 127, p. 227.
[15] G.H. Kühl, J. Phys. Chem. Solids 38 (1977) 1259.
[16] F. Roessner, K.-H. Steinberg, A. Rudolf and B. Staudte, Zeolites 9 (1989) 371.
[17] A. Kogelbauer, J.A. Lercher, K.-H. Steinberg, F. Roessner, A. Soellner and R.V. Dmitriev, Zeolites 9 (1989) 224.
[18] T. Fleckenstein, K. Belendorff and F. Fetting, Chem. Ing. Techn. 57 (1985) 800.